ELSEVIER

J. Non-Newtonian Fluid Mech. 99 (2001) 183–201

Journal of Non-Newtonian Fluid Mechanics

www.elsevier.com/locate/jnnfm

Recirculating turbulent flows of thixotropic fluids

A.S. Pereira [a], F.T. Pinho [b,*]

[a] *Departamento de Engenharia Química, Instituto Superior de Engenharia do Porto, Rua de São Tomé, 4200 Porto, Portugal*
[b] *Centro de Estudos de Fenómenos de Transporte, DEMEGI, Faculdade de Engenharia, Universidade do Porto, Rua Dr. Roberto Frias, 4200-465 Porto, Portugal*

Received 22 January 2001; received in revised form 28 March 2001

Abstract

An aqueous suspension of 1 wt.% laponite was investigated in terms of its rheology and hydrodynamic behaviour in a sudden expansion flow. The fluid was shear-thinning, thixotropic and had an yield stress which was measured by direct and indirect methods. The oscillatory tests showed that the elasticity of the 1% laponite suspension was very small.

The high Reynolds number flow downstream of a sudden expansion, with fully-developed inlet conditions, showed no major difference in relation to the flow of water. There were no differences between the mean and turbulent flow characteristics of the water and laponite flows upstream and downstream of the expansion plane, except for a small anticipation of the loci of maximum Reynolds stresses with the suspension, which had no further consequence. In conclusion, the laponite suspension flows were akin to those of water.

Keywords: Thixotropy; Shear-thinning; Viscoplasticity; Laponite suspension; Turbulent sudden expansion flow

1. Introduction

In the chemical and processing industries, such as the cosmetic and pharmaceutical industries or the cleaning, agriculture, building or paper industries to name but a few, there are often non-Newtonian fluids that exhibit a shear-thinning viscosity in combination with an yield stress, elasticity and thixotropy. Fluids having these characteristics are also encountered as drilling fluids and this has been one of the relevant motivations for the virtually hundreds of papers on their rheology (see the 20 years old review of Mewis [1]). In many of these applications, and within the manufacture of these products, either pumping (pipe flow) or separated flows (recirculation within stirred reactors, for instance) take place, and if the fluids are highly shear-thinning, the flows can easily attain turbulent conditions. Typically, such fluids are made from different components, such as polymer molecules and solid particles, with the latter usually imparting a time-dependent behaviour.

* Corresponding author.
E-mail address: fpinho@fe.up.pt (F.T. Pinho).

0377-0257/01/$ – see front matter
PII: S0377-0257(01)00117-3

The flow of these fluids is necessarily complex and still requires a significant amount of investigation to be better understood. Although there is a wealth of literature on the rheology of thixotropic fluids, the same does not apply to the study of their hydrodynamics, especially regarding flows other than the simpler pipe and channel flows. Simplicity, here is purely geometrical and apparent, because a quick review of the scarce literature in the field [2] immediately shows that duct flows of thixotropic fluids are everything but simple.

In turbulent flow research, an improved understanding of flows benefits from their classification into typical classes [3]. Two of the main types of turbulent flows are those where turbulence is dominated by the proximity to a wall, such as the above mentioned pipe and channel flows, or wall-free flows, such as those in jets or mixing layers. Within this latter group on external flows one typical situation is that of recirculating flows, which combine characteristics of both wall and wall-free flows at different locations.

Recirculating flows are extremely common in industrial situations: they appear downstream of many fittings or accessories in piping systems, in stirred reactors or heat exchangers, and thus it is essential that we understand their flow characteristics in order to improve the design of processing equipment. For Newtonian fluids, there is a wealth of literature (see, for instance [4–6]), because recirculating flows are common in many other relevant industrial situations, such as in combustion, but for non-Newtonian fluids the literature is scarcer (see [7,8]) and within this field the authors are unaware of anything involving thixotropic fluids.

One of the reasons for the scarcity of literature on fluid dynamics of thixotropic fluids has to do with the difficulties of operation with these fluids. First, since they usually contain solid particles, which are responsible for their thixotropy, they are frequently opaque and this severely limits the scope of experimental techniques. For opaque fluids ultrasound devices can be used, but they lack spatial resolution for accurate measurements of turbulent flow and the new and more promising nuclear magnetic resonance [9] is still far too expensive, and consequently not yet widely available. The alternative for accurate diagnostics is the use of optical techniques, but this requires transparent fluids. Secondly, their relevant rheological properties, such as the viscosity, keep changing with time and this makes it extremely difficult to ensure reproducibility of results and fluid properties, or even to select the adequate quantities that will be used to normalise the results.

One clay that is used as an additive in drilling muds, and has the advantage of transparency when suspended in water, is laponite. It is a synthetic product which alone, or in combination with a polymer such as carboxymethyl cellulose (CMC), produces fluids that have variable degrees of viscoelasticity, thixotropy, shear-thinning and viscoplasticity. Aqueous suspensions of laponite are in fact considered as model fluids in various types of rheological and hydrodynamic experiments, because of their excellent clarity, which is due to high purity and small particle size. Other advantages are their non-toxicity, indefinite shelf life, and incapacity to sustain bacterial growth [10,11].

Turbulent flow research with slurries has been generally limited to investigations of pipe flow, such as the LDA measurements of Park et al. [12] with an oil-based transparent slurry with yield stress obeying the Herschel–Bulkley law and the more recent investigations of Escudier and co-workers [2,13]. Escudier and Presti [2] and Escudier et al. [13] used transparent aqueous suspensions based on laponite and a mixture of laponite and a polymer, respectively. Park et al. used silica particles suspended in a mixture of Stoddard solvent and mineral oil and reported a time-independent fluid with yield stress, which followed theory in laminar flow, and a behaviour similar to that of Laufer [14] in the turbulent regime. A major difference between the two sets of works on pipe flow concerns the fluid rheology in respect to time dependence. For both cases, shear-thinning yield stress fluids obeying the Herschel–Bulkley law were

selected, but whereas in Park et al., the fluid was time independent, the laponite suspensions exhibited thixotropy. In Escudier and Presti [2], the flowfield of 1.5% laponite suspensions was investigated in detail in the laminar, transitional and turbulent flow regimes. They concluded that laminar flow was accurately predicted by the Herschel–Bulkley model fitted to viscosity data at the prevailing flow conditions rather than the equilibrium state used in rheological characterisation, and that the transition Reynolds number was similar to that for Newtonian fluids. In turbulent flow, the laponite suspensions exhibited drag reduction, but less than usually found with polymer solutions, and reduced transverse turbulence relative to that of Newtonian flows.

As mentioned above, we are unaware of literature on recirculating flows with thixotropic fluids. For time-independent, shear-thinning, viscoelastic fluids, however, there has been some work by Pak et al. [15,16], Pinho and co-workers [7,17,18] as well as by Escudier and Smith [8]. In fact, the recent papers of Escudier and Smith [8] and Pereira and Pinho [17] are complementary and investigate the flow of xanthan gum (XG) solutions in order to assess the effects of polymer concentration, Reynolds number and especially of the inlet conditions. This has just been extended to the study of the expansion ratio effect by Pereira and Pinho [18].

Clearly, we do not know how a thixotropic fluid behaves in recirculating turbulent flows and this paper is aimed at initiating such research. Here, we present results of the sudden expansion flow of a suspension of laponite and compare the results with those of water in the same geometry. The sudden expansion is axisymmetric, from 26 to 40 mm diameter, the inlet flow is fully-developed, and the results are analysed in view of the rheology of the laponite suspension and the turbulent pipe flow characteristics obtained previously [19].

The remaining of this report is organised as follows: first, the experimental facilities and instrumentation are described and this is followed by the rheological characterisation of the fluids. The overall and mean flow characteristics of the sudden expansion flow are then presented and discussed and are followed by the corresponding turbulent flowfield analysis after which the paper ends with the main conclusions.

2. Experimental setup and instrumentation

2.1. The rig, pressure transducers and flowmeter

The hydrodynamic measurements were carried out in the flow rig described in Castro and Pinho [7] and represented schematically in Fig. 1. Fluid was pumped from a 120 l tank through a rising pipe and then through the 90 diameter long descending pipe, the test section and the final pipe leading to the tank. The vertical, descending pipe located upstream of the test section had a constant 26 mm inside diameter and ensured that the flow was fully-developed prior to the sudden expansion. The test section was made of acrylic and initially it also had an internal diameter of 26 mm, which expanded suddenly to a pipe of 40 mm. The expansion test section was 430 mm long and a further 700 mm long pipe of 40 mm diameter led the fluid back to the tank. The test section had a square outer cross-section in order to reduce refraction of laser beams.

The flow was controlled by two valves and one by-pass circuit, and a 100 mm long star-shaped honeycomb was located at the inlet of the descending pipe to help ensure a fully-developed flow at the inlet of the test section. Heating and cooling circuits in the reservoir were used to control and maintain the temperature at a constant $25 \pm 0.5^{\circ}C$.

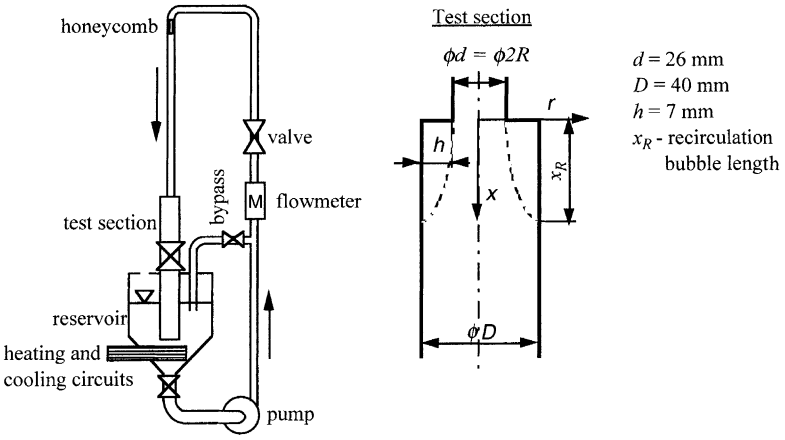

Fig. 1. Schematic representation of the rig, test section and co-ordinate system.

The sudden expansion test section had 18 pressure taps downstream of the expansion plane and two taps upstream, in the inlet region of 26 mm diameter where the flow was fully-developed. Pressure differences were measured by means of two differential pressure transducers, models P305D-S20 and P305D-S24 from Valydine, and the flowrate was measured by an electromagnetic flowmeter Mag Master from ABB Taylor, which was incorporated in the rising pipe, 15 diameters downstream of the closest flow perturbation. All these instruments were connected to a 386 PC by a data acquisition Metrabyte DAS-8 board interfaced with a Metrabyte ISO-4 multiplexer, both from Keithley.

The flowmeter was capable of measuring the volumetric flowrate in the range 0–5 l/s with an accuracy of 0.2% of full scale. As a further check to its accuracy, the velocity profile measurements carried out by LDA were integrated and the computed flowrate never differed by more than 1% from the output of the flowmeter.

All pressure taps were drilled carefully to avoid the appearance of spurious edge effects, and had the same geometry so that any systematic errors would cancel out in the pressure difference measurement. The recommendations of Shaw [20] and Franklin and Wallace [21] for the design of pressure taps and the quantification of pressure measurement errors were followed and it was estimated that the associated contribution to the overall uncertainty was $<1.5\%$ at a high Reynolds number flow. Taking into account the other sources of uncertainty, such as accuracy of the transducers, calibration errors, zero drift effects and statistics, the total uncertainty of the pressure difference measurements was estimated, by application of the RMS equation, to vary between 1.6 and 7.2% at low and high flowrates, respectively.

2.2. The laser–Doppler anemometer

A fibre optics laser–Doppler velocimeter from INVENT, model DFLDA, was used for the velocity measurements with a 30 mm probe mounted on the optical unit. Scattered light was collected by a photo diode in the forward scatter mode, and the main characteristics of the anemometer are listed in Table 1 and are described by Stieglmeier and Tropea [22]. The signal was processed by a TSI 1990C counter interfaced with a computer via a DOSTEK 1400 A card, which provided the statistical quantities. The data presented in this paper have not been corrected for the effects of the mean gradient broadening. The

Table 1
Laser–Doppler characteristics

Laser wavelength (nm)	827
Laser power (mW)	100
Measured half angle of beams in air	3.68
Dimensions of measuring volume in water at e^{-2} intensity	
Minor axis (μm)	37
Major axis (μm)	550
Fringe spacing (μm)	6.44
Frequency shift (MHz)	2.5

maximum uncertainties in the core of the flow downstream of the expansion, at a 95% confidence level, were of 1 and 2.2% for the axial mean and RMS velocities, respectively and of 2.5% for the radial and tangential RMS velocities. In the mixing layer and in the recirculating region the maximum uncertainties are higher, of the order of 1.3 and 5.2% for the axial mean and RMS velocities, respectively and of 5.3% for both the radial and tangential RMS velocity components.

The refraction of the beams at the curved optical boundaries was taken into account in the calculations of the measuring volume location, measuring volume orientation and conversion factor, following standard refraction equations presented in Durst et al. [23]. For measurements of the radial component of the velocity, the plane of the laser beams was perpendicular to the test section axis and the anemometer was traversed sideways, in the normal direction relative to the optical axis.

The velocimeter was mounted on a three-dimensional milling table and the positional uncertainties are those of Table 2. The positioning of the control volume was done visually with the help of infrared sensitive screens, video camera and monitor. Any systematic positional error was corrected by plotting the axial mean velocity profiles, and whenever the asymmetry of the flow was greater than half the size of the control volume, that value was added or subtracted to the milling table so that the profile became symmetric. This method was verified by measuring a second time the same velocity profile and seen to produce always a symmetric curve after the correction was applied. This verification was always carried out prior to the measurements of the transverse velocity components.

2.3. The rheometer

The rheological characterisation of the fluids was carried out in a rheometer from Physica, model Rheolab MC 100, made up of an universal measurement unit UM/MC fitted with the low viscosity

Table 2
Estimates of positional uncertainty

Quantity	Systematic	Random (μm)
r (Horizontal plane) accuracy of milling table	–	±10
x (Vertical) accuracy of milling table	–	±100
r (Horizontal plane) accuracy of visual positioning	–	±200
x (Vertical) accuracy of visual positioning	–	±100

double-gap concentric cylinder Z1-DIN system. Following the recommendations of the manufacturer, this geometry was adequate to measurements of these low viscosity suspensions because the gap size was more than 20 times the size of the larger particles [24] and it allowed the measurement of viscosities between 1 and 67.4 mPa at the maximum shear rate of 4031 s^{-1}. The rheometer could be both stress and shear rate controlled, a possibility that was used according to the ranges of viscosity and shear rate under observation. A thermostatic bath and temperature control system, Viscotherm VT, allowed the control of temperature of the fluid sample at 25°C within ±0.1°C.

The rheometer was operated in steady state to measure the viscometric viscosity, in oscillatory flow to measure the elastic and viscous components of the dynamic viscosity, and creep tests were also carried out in an attempt to quantify the fluid elasticity and viscoplasticity in the wider possible manner. In the viscometric viscosity runs at low shear rates, the rheometer was operated in the controlled shear stress mode, and the uncertainty of the measurements was better than 3.5%, whereas at higher shear rates the shear rate control mode was used and the uncertainty was better than 2%. For the creep tests, the uncertainty was better than 5 and 10% for high and low shear stresses, respectively.

3. Fluid characterisation

3.1. The fluids

Aqueous suspensions of 1% w/w of laponite RD were produced for investigation in this work. Laponite RD is a synthetic smectite clay manufactured by Laporte Industries. Its structure is analogous to that of the natural mineral clay hectorite, but with a smaller size. It is a layered hydrous magnesium silicate which is hydrothermally synthesised from simple silicates and lithium and magnesium salts, in the presence of mineralising agents. Further details of the chemical structure of laponite, its production and applications can be found in [24,25].

The fluids were always prepared following the same procedure, and using Porto tap water, in a tank of 130 l of capacity. To prevent bacteriological degradation, 100 ppm of formaldehyde was added and 60 ppm of sodium chloride increased the yield stress of the solutions. More than 100 l of fluid were required to fill the sudden expansion rig, and the solutions were mixed for 90 min and settled for more than 24 h to allow complete hydration of the interstitial spaces between the clay particles. Before the rheological characterisation of the suspensions and/or its transfer to the flow rig, the suspensions were mixed for 30 min to full homogenisation.

3.2. Viscometric viscosity

The laponite suspensions are shear-thinning and have an yield stress. Since they are also thixotropic, a flow-equilibrium test procedure was adopted to measure the viscometric viscosity. The equilibrium procedure was established by Alderman et al. [26] whereby a shear is applied to the fluid sample and the shear rate monitored until steady state conditions are achieved. Only then is the viscosity reading performed. The rheological behaviour of a wider range of laponite suspensions was investigated in [19] and there it was found that a time span of the order of 3000 s was required to attain an equilibrium state.

Following this procedure, the viscosity curve of Fig. 2 was obtained which corresponds to the final equilibrium states for a wide range of shear stresses/rates of the 1% laponite suspension. The suspension

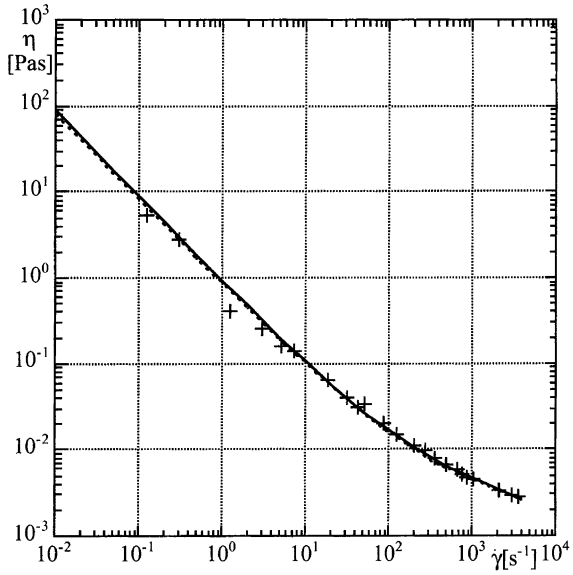

Fig. 2. Viscometric viscosity of the 1% laponite suspension in the equilibrium state. Lines represent fitting by models — full line: Herschel–Bulkley; dashed line: Casson.

exhibits a strong shear-thinning behaviour without the Newtonian plateau at low shear rates, as is typical of fluids possessing an yield stress. At high shear rates, the viscosities are rather low, just of the order of three times the viscosity of the solvent.

The solid line in Fig. 1 represents the fit of the data by the Herschel–Bulkley model,

$$\eta = \frac{\tau_{\mathrm{HB}}}{\dot{\gamma}} + K\dot{\gamma}^{n-1}, \tag{1}$$

whose parameters are $n = 0.685$, $K = 0.033\,\mathrm{Pa}^{0.685}$ and $\tau_{\mathrm{HB}} = 0.9\,\mathrm{Pa}$, and the dashed line represents the fit by the Casson model,

$$\eta = \frac{\tau}{\dot{\gamma}} \quad \text{with} \quad \sqrt{\tau} = \sqrt{\tau_{\mathrm{Cas}}} + \sqrt{\tau_\infty \dot{\gamma}}, \tag{2}$$

which gave $\tau_{\mathrm{Cas}} = 0.8\,\mathrm{Pa}$ and $\eta_\infty = 0.00146\,\mathrm{Pa}$.

3.3. Oscillatory shear flow

Measurements of the storage (G') and loss (G'') modulli in oscillatory shear flow were also carried out, but the maximum shear amplitude for linear behaviour was so small that accurate results were difficult to obtain. The ratio G'/G'' of the 1% laponite suspension was rather small, of about 0.12 for frequencies in the range 1–5 Hz and of 0.14 between 5 and 10 Hz, suggesting low elasticity. As was seen by Pereira and Pinho [19], this fluid is significantly less elastic than a pure 1.5% laponite suspension and a laponite/CMC blend, and so it constitutes a good option for assessing the effects of shear-thinning, thixotropy and yield stress upon flow characteristics, without the added complexity of fluid elasticity.

Table 3
Yield stress values obtained by the various methods[a]

Solution	τ_c	τ_s	τ_{Cas}	τ_{HB}
1% Laponite	1.8	1.7	0.8	0.9

[a] τ_c: creep; τ_s: increasing stress; τ_{Cas}: Casson model fitting; τ_{HB}: Herschel–Bulkley model fitting.

3.4. Yield stress

Yield stress is sensitive to the duration and type of test procedure [27] and especially so for time-dependent fluids, as in this work. Measurements of the yield stress were carried out using standard direct and indirect procedures: the direct techniques were the creep test and the increasing stress test defined by the American Petroleum Institute (API) [28], whereas the indirect methods were the extrapolation of the equilibrium viscosity data by known rheological models.

In the creep test, increasing values of the shear stress were applied to the fluid sample for a period of time and then the stress was removed. When the applied stress was higher than the yield stress, there was a final deformation at the end of the experiment. The test is described in more detail in [19] and resulted in a yield stress value of 1.9 Pa.

For the increasing stress test of API, the yield stress was the maximum stress value measured, and interpreted by Liddell and Boger [29] as the stress marking the transition between the viscoelastic and purely viscous behaviour. However, the time resolution of our rheometer was not sufficient for a clear maximum stress to be observed and consequently the result from this test ($\tau_s = 1.7$ Pa) should be regarded with caution.

As indirect methods, the equilibrium viscosity data were fitted by the Herschel–Bulkley (Eq. (1)) and Casson (Eq. (2)) models which gave $\tau_{HB} = 0.9$ Pa and $\tau_{Cas} = 0.8$ Pa, respectively.

The results of the various direct and indirect measurements of the yield stress are summarised and compared in Table 3. There is clearly a difference between the indirect results, of about 0.9 Pa, and those obtained through the direct procedures, which are twice as large.

The values of yield stress obtained by different measuring techniques must necessarily be different; whereas the creep test measures the yield stress, without destroying the inner structure of the fluid sample, the indirect measurements rely on a procedure that requires a different, less ordered state of dynamic equilibrium which, consequently, lead to lower values.

From a critical assessment of the set of results one may conclude that the yield stress values of relevance to these hydrodynamic results are those obtained from dynamic equilibrium experiments, i.e. the indirect values of 0.9 Pa.

4. Results and discussion

4.1. Initial considerations

In the sudden expansion test section, measurements were performed of the three components of the mean and RMS of the fluctuations of the velocity and also of the longitudinal variation of the pressure coefficient for the 1% laponite suspension. The expansion had a diameter ratio of $D{:}d = 1.538$ and the

Table 4
Flow conditions, recirculation length and maximum turbulent quantities in the $D{:}d = 1.538$ sudden expansion

Run	Fluid	U_1 (m/s)	Re	Re_w	Re_{gen}	x_R/h	$(\overline{u'^2}/U_1^2)_{max}$	$(\overline{v'^2}/U_1^2)_{max}$	$(\overline{w'^2}/U_1^2)_{max}$	$(k/U_1^2)_{max}$
1[a]	Water	4.61	135000	135000	135000	8.43	0.0466	0.0275	0.0326	0.0533
2[a]	Water	1.73	50300	50300	50300	8.71	0.0422	0.0270	0.0279	0.0478
3	1% Laponite	4.57	21250	99540	9270	8.57	0.0430	0.0241	0.0296	0.0475
4	1% Laponite	3.07	11690	48160	4840	8.71	0.0410	0.0213	0.0292	0.0437

[a] From [17].

results will be compared with those obtained by Pereira and Pinho [17] for water, in the same test section. The inlet flow conditions were the same, namely, fully-developed flow, and Table 4 summarises and compares the main flow characteristics: inlet bulk flow velocity U_1, three different Reynolds numbers, recirculation length and maximum values of the three normal Reynolds stresses and turbulent kinetic energy downstream of the expansion plane.

The three Reynolds numbers used to characterise the flow conditions are

1. the upstream pipe Reynolds number

$$Re_w = \frac{\rho U_1 d}{\eta_w}, \tag{3}$$

   where U_1, d and η_w are the bulk velocity, pipe diameter and wall viscosity, respectively, all referred to the upstream pipe. The wall viscosity is obtained from the rheogram and the measurement of the pressure drop in the upstream fully-developed flow;
2. the upstream pipe generalised Reynolds number

$$Re_{gen} \equiv \frac{\rho U_1^{2-n} d^n}{K}, \tag{4}$$

   where K and n represent the consistency and power indices of an Ostwald de Waele power law fitting to the viscosity data plotted in Fig. 2;
3. the Reynolds number Re presented by Castro and Pinho [7]

$$Re \equiv \frac{\rho U_1 d}{\eta_{ch}}, \tag{5}$$

   where the characteristic viscosity η_{ch} is obtained from the rheogram at a characteristic value of the shear rate $\dot{\gamma}_{ch}$ of

$$\dot{\gamma}_{ch} \equiv \frac{U_1}{h}, \tag{6}$$

   with h representing the step height.

From Table 4, we observe that there are basically no differences in recirculation length between the water and the 1% laponite flows, except those related to a small Reynolds number effect. There are some differences on the maximum values of the normal Reynolds stresses and on the turbulent flowfields but, as we shall see, these are not strong enough to affect the mean flow.

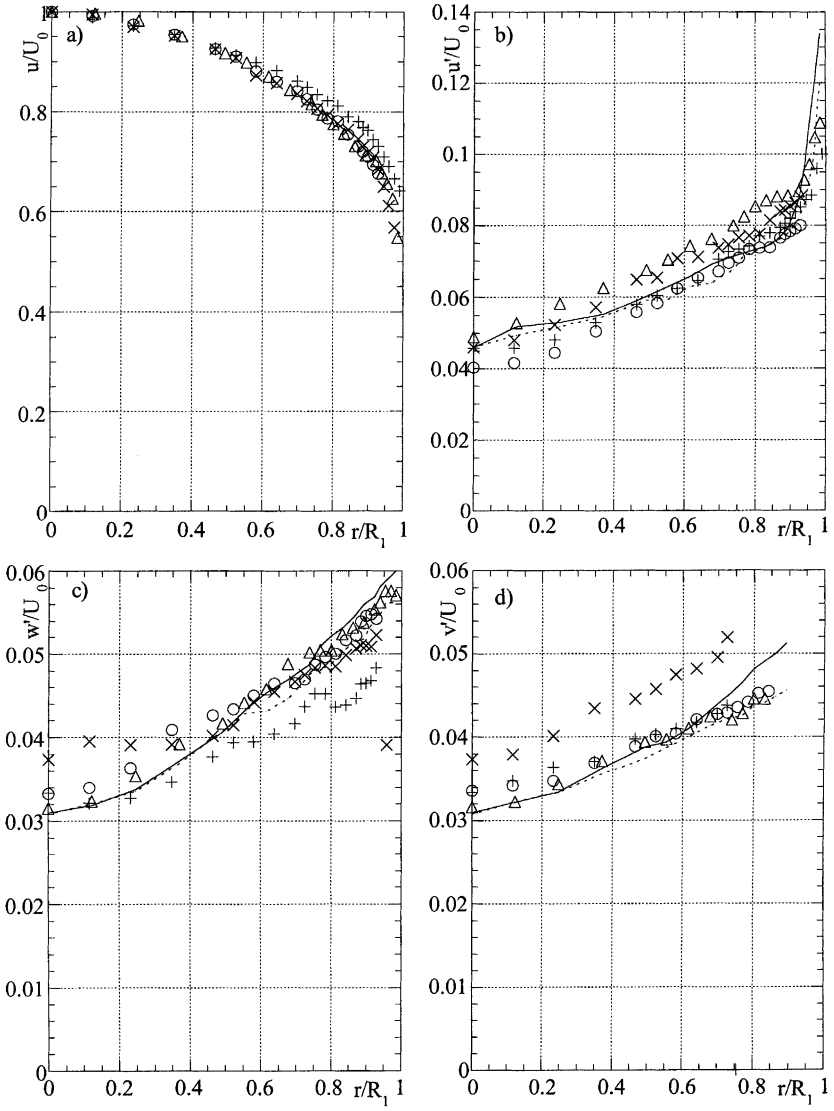

Fig. 3. Radial profiles of the inlet mean and turbulent flow conditions at $x/d = -0.5$: (×) water $Re = 50{,}300$; (+) water $Re = 135{,}000$; (△) 1% laponite $Re_w = 48{,}160$; (○) 1% laponite $Re = 99{,}540$; full line 1% laponite pipe flow data $Re_w = 37{,}200$ from [19]; dashed line 1% laponite pipe flow data $Re_w = 102{,}700$ from [19]. (a) u/U_0 (b) u'/U_0; (c) w'/U_0; (d) v'/U_0.

4.2. Inlet flow

In the sudden expansion test section, the inlet flow was measured at $0.5d$ upstream of the expansion plane, with d representing the diameter of the upstream pipe. Transverse profiles of the axial mean velocity and of the RMS of the three fluctuating velocity components are shown in Fig. 3 after normalisation with the centreline velocity. The Newtonian data, when normalised with the friction velocity, compared favourably with the data from the literature [14,30,31]. The mean velocity profiles are very similar,

with the Newtonian flow at a Reynolds number of 135,000 showing a flatter profile than the laponite flow.

The Newtonian and laponite turbulent profiles are all very similar, exhibiting scatter of the same order of magnitude as seen in the data of Laufer [14], Lawn [30] and Townes et al. [31]. Fig. 3(b–d) also compare the inlet data of the 1% laponite suspension with profiles measured with the same fluid in a straight pipe and presented by Pereira and Pinho [19]. In that work both the water and the 1% laponite profiles agree with Clark's [32] log-law when plotted in wall co-ordinates. Clearly, both sets of data are similar, which rules out any upstream flow effect upon events taking place downstream of the expansion plane. It is important to emphasise at this stage that in their sudden expansion investigations, Pereira and Pinho [17] observed higher axial wall turbulence and lower radial and tangential turbulence with polymer solutions than with water at the inlet pipe. These differences are not observed here when comparing laponite and water and this will have implications in the downstream flow characteristics.

4.3. Expansion mean flow

In Pereira and Pinho [17], these same water flow measurements were seen to compare favourably with literature data on Newtonian sudden expansion flows. There and also in the recent work of Pereira and Pinho [18], the behaviour of aqueous solutions of XG were investigated for different expansion ratios and Reynolds numbers, and it was reported that polymer solutions reduced the recirculation length relative to that of Newtonian fluids. On the contrary, the pure 1% laponite suspension exhibits no difference relative to the water flow, as inspection of Table 4 shows and the data to be presented below further confirms.

The detailed measurements of the axial velocity component allow the determination of the vorticity thickness (δ_ω) and its axial variation. The vorticity thickness is defined as

$$\delta_\omega \equiv \frac{U^+ - U^-}{(\partial u/\partial r)_{\max}}, \tag{7}$$

where U^+ and U^- represent the local maximum and minimum velocities in the shear layer, here assumed to be the centreline velocity U_0 and 0, respectively.

Fig. 4 represents the axial variation of the vorticity thickness, normalised by the upstream pipe diameter, and again the water and laponite flows show very similar behaviour. A line fit, expressed by Eq. (8), represents well the variation of the normalised vorticity thickness for all fluids. This variation is similar to that reported in the earlier work of Pereira and Pinho [17].

$$\frac{\delta_\omega}{d} = 0.155\frac{x}{d} + 0.107. \tag{8}$$

Fig. 5 compares the downstream mean flowfields of the 1% laponite suspension with those of the water flows. The lines in the figures represent the location of zero axial mean velocity. The mean flows are similar, except in the mixing layer just downstream of the expansion plane. There, a slight delay in flow development of the low Reynolds number flow of 1% laponite is seen and this results in slightly higher mean velocity gradients. Downstream of the reattachment region, the flow is redeveloping and the profiles of water tend to be flatter.

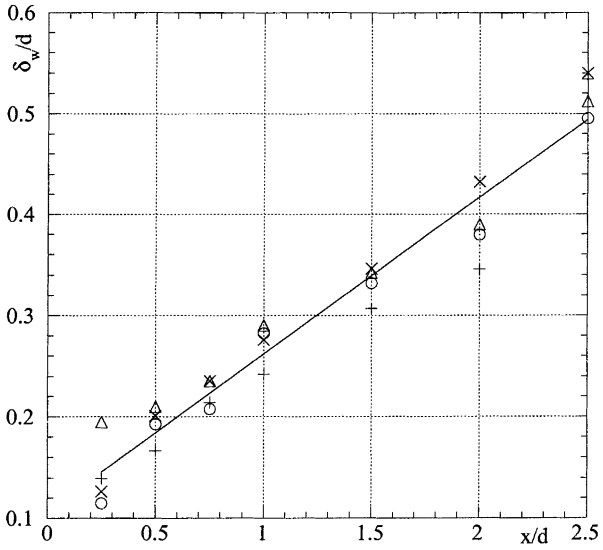

Fig. 4. Longitudinal variation of the vorticity thickness: (×) water $Re = 50{,}300$; (+) water $Re = 135{,}000$; (△) 1% laponite $Re_w = 48{,}160$; (○) 1% laponite $Re_w = 99{,}540$; full line: Eq. (8).

The measurements of wall static pressure allowed the determination of the static pressure variation coefficient (Eq. (9)), which is plotted as a function of x/d in Fig. 6.

$$C_T \equiv \frac{p - p_0}{(1/2)\rho U_{in}^2}. \tag{9}$$

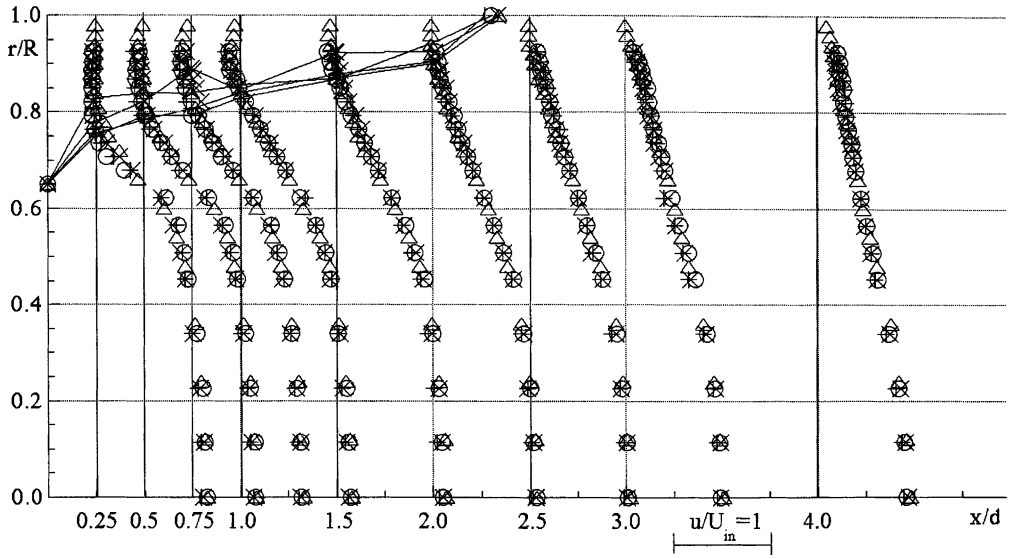

Fig. 5. Normalised mean velocity profiles: (×) water $Re = 50{,}300$; (+) water $Re = 135{,}000$; (△) 1% laponite $Re_w = 48{,}160$; (○) 1% laponite $Re_w = 99{,}540$.

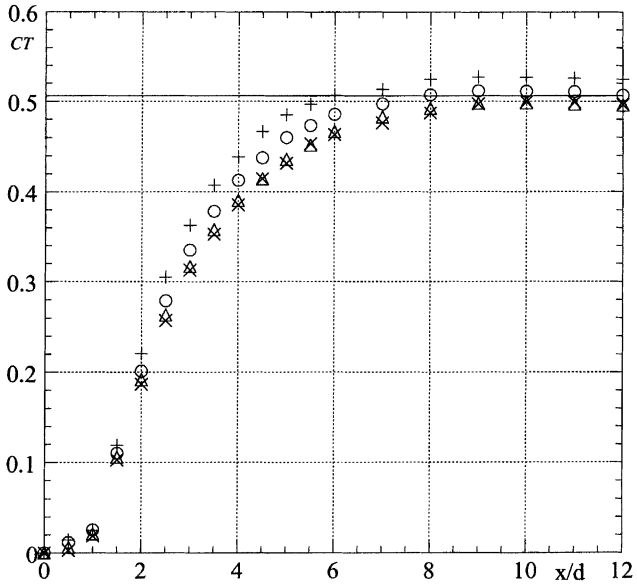

Fig. 6. Longitudinal variation of the static pressure coefficient: (×) water $Re = 50{,}300$; (+) water $Re = 135{,}000$; (△) 1% laponite $Re_w = 48{,}160$; (○) 1% laponite $Re_w = 99{,}540$; (—) Eq. (10) with $\beta_1 = \beta_2 = 1.036$ (average value from Table 5).

In Eq. (9), p_0 is the reference pressure measured in the last tap of the upstream pipe, just upstream of the sudden expansion plane. The curves of C_T are again fairly similar and show recovery taking place at around $x/d \approx 9$–10, with values of C_T in close agreement with each other and with the result of an inviscid analysis.

The inviscid analysis shows the theoretical static pressure coefficient C_T to be given by

$$C_T = \beta_1 \sigma \left(1 - \frac{\beta_2}{\beta_1}\sigma\right), \tag{10}$$

and its derivation can be found in the literature, one recent example being Oliveira and Pinho [33]. In Eq. (10), $\sigma = (d/D)^2$ and β_1 and β_2 are fully-developed momentum shape factors upstream and downstream of the expansion ($\beta \equiv \overline{u^2}/\bar{u}^2$, where the overbar denotes area average). The upstream momentum shape factors were determined from the mean velocity profiles measured at $x/d = -0.5$ and are listed in Table 5.

Table 5
Momentum shape factor β_1 in the fully-developed upstream profile measured at $x/d = -0.5$ and corresponding C_T assuming $\beta_1 = \beta_2$

Fluid	Re_w	β_1	C_T
Water[a]	134000	1.033	0.504
Water[a]	50400	1.039	0.507
1% Laponite	99540	1.036	0.506
1% Laponite	48160	1.039	0.507

[a] From [17].

The static pressure variation coefficient is rather sensitive to β_1: the theoretical value of C_T, for uniform inlet and outlet profiles ($\beta = 1$), is 0.488, which is raised by an average 3.7% when the true value of β_1 is considered and it is assumed that the downstream fully-developed profile has the same shape as the upstream profile. This is probably true for all the flows here, except for a small effect of Reynolds number: although that would not be the case for polymer solutions, which have a drag reducing behaviour that depends on pipe diameter, the 1% laponite suspension was seen by Pereira and Pinho [19] to behave in a pure viscous way for wall Reynolds numbers above 35,000. Thus, it is possible that in a 40 mm diameter pipe, the same suspensions would still behave similarly, i.e. in a purely viscous faction. Accordingly, we assumed $\beta_2 = \beta_1$, but even if that was not the case the equality remained a good assumption, because C_T is not so sensitive to β_2/β_1.

The horizontal line in Fig. 6 represents the theoretical C_T for $\beta_1 = 1.036$. In all cases, the measured C_T differs from this theoretical C_T only by a small amount, because of the role of the wall shear stresses and of experimental uncertainties which are absent from the theoretical expression. Once again, but this time through the pressure variation, the picture is of similarity between the Newtonian and the pure laponite flowfields.

4.4. Expansion turbulent flow

Figs. 7–9 show radial profiles of the normalised axial, tangential and radial Reynolds stresses at some representative cross-stream planes downstream of the expansion, respectively. For all fluids, the axial normal stress is the highest, followed by the tangential and radial stresses. In almost all profiles, the Newtonian flow at $Re = 135{,}000$ shows slightly higher peak stresses in agreement with the differences in maximum values listed in Table 4. The loci of the maximum values of each Reynolds stress are close to each other for all flows, well within the shear layer, at an average location of $r/R = 0.7$ and $x/d = 2$. Inspection of contour plots and other radial profiles, not shown here for compactness, indicate that for the tangential, and especially the radial components, the loci of maximum Reynolds stress for the laponite suspensions are slightly anticipated to about $x/d \approx 1.8$–1.9. The overall picture is that differences in the values of turbulence are small and that the turbulent flowfields are quite similar, with the small differences having no impact upon the mean flowfield, in contrast to observations made by [17,18] involving aqueous solutions of the highly drag reducing XG.

In Pereira and Pinho [17,18], the differences between the Newtonian and XG mean and turbulent flowfields up to reattachment were basically the outcome of different turbulent inlet conditions, which in the present case are absent as seen in Section 4.2. Those differences in upstream turbulence were advected downstream and resulted in peak values of turbulence occurring earlier than those of the water flows, with the consequent higher rates of momentum transfer at the initial stages of the expansion flow and a reduced recirculation length. The differences in upstream turbulence between the laponite and Newtonian flows are negligible and of the same order of those reported in the fully-developed pipe flow investigated by the same authors [19]. As a consequence, the stronger anticipation of turbulence stress maxima seen with polymer solutions does not take place with laponite, and the turbulent flowfields of water and laponite develop similarly.

A second difference between the XG and Newtonian flows in Pereira and Pinho [17,18] was the higher turbulent kinetic energy dissipation which resulted in a stronger dampening of the turbulence of XG downstream of reattachment. That picture was consistent with the relative behaviour of Newtonian and XG solutions in fully-developed pipe flows. The more intense dissipation of turbulent kinetic energy seen

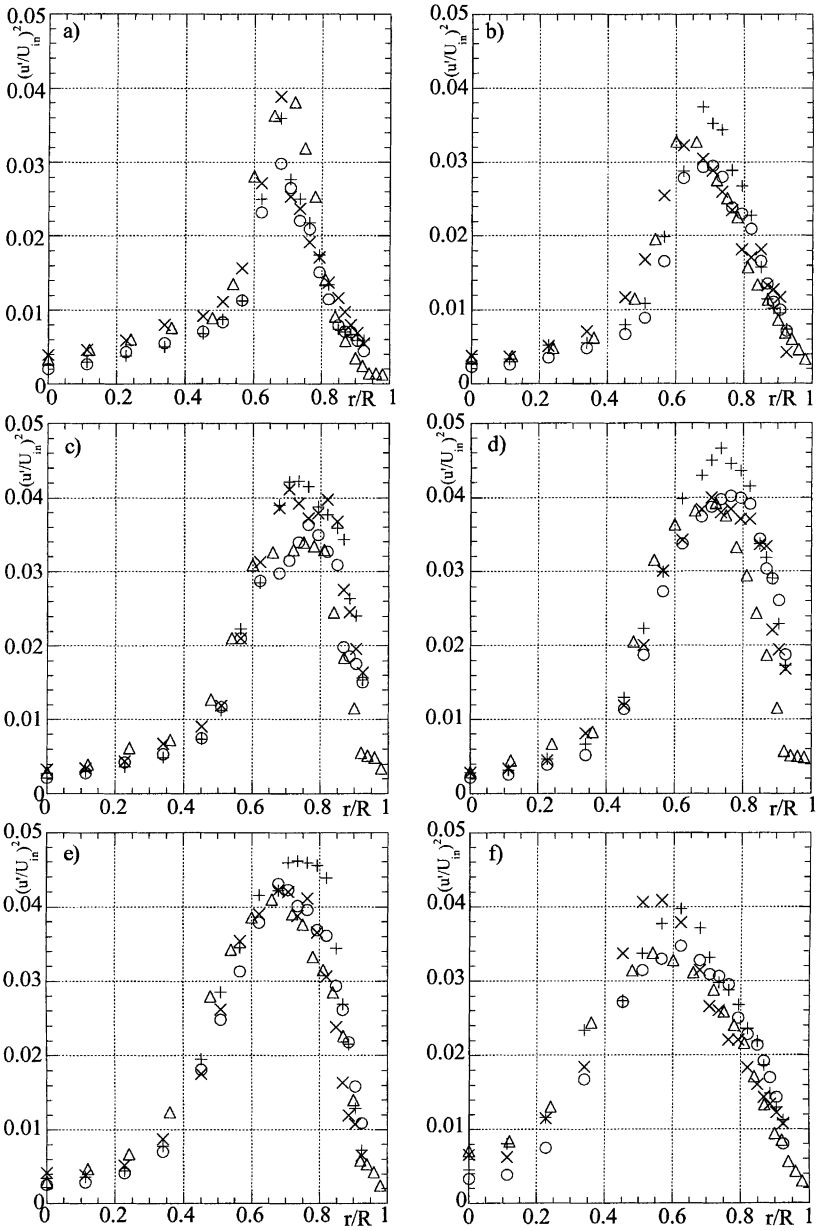

Fig. 7. Transverse profiles of the axial normal Reynolds stress downstream of the expansion for (×) water $Re = 50{,}300$; (+) water $Re = 135{,}000$; (△) 1% laponite $Re_w = 48{,}160$; (○) 1% laponite $Re_w = 99{,}540$ at $x =$ (a) $0.5d$; (b) $0.75d$; (c) $1.0d$; (d) $1.5d$; (e) $2.0d$; (f) $3.0d$.

with the XG solutions is also absent from the laponite suspensions, otherwise the profiles at $x/d = 3$ would already show significant differences between the laponite and water flows. This is also consistent with the fully-developed pipe flow findings of Pereira and Pinho [19], where the intense dampening of the transverse turbulence, so typical of highly drag reducing fluids, is absent from the laponite flows.

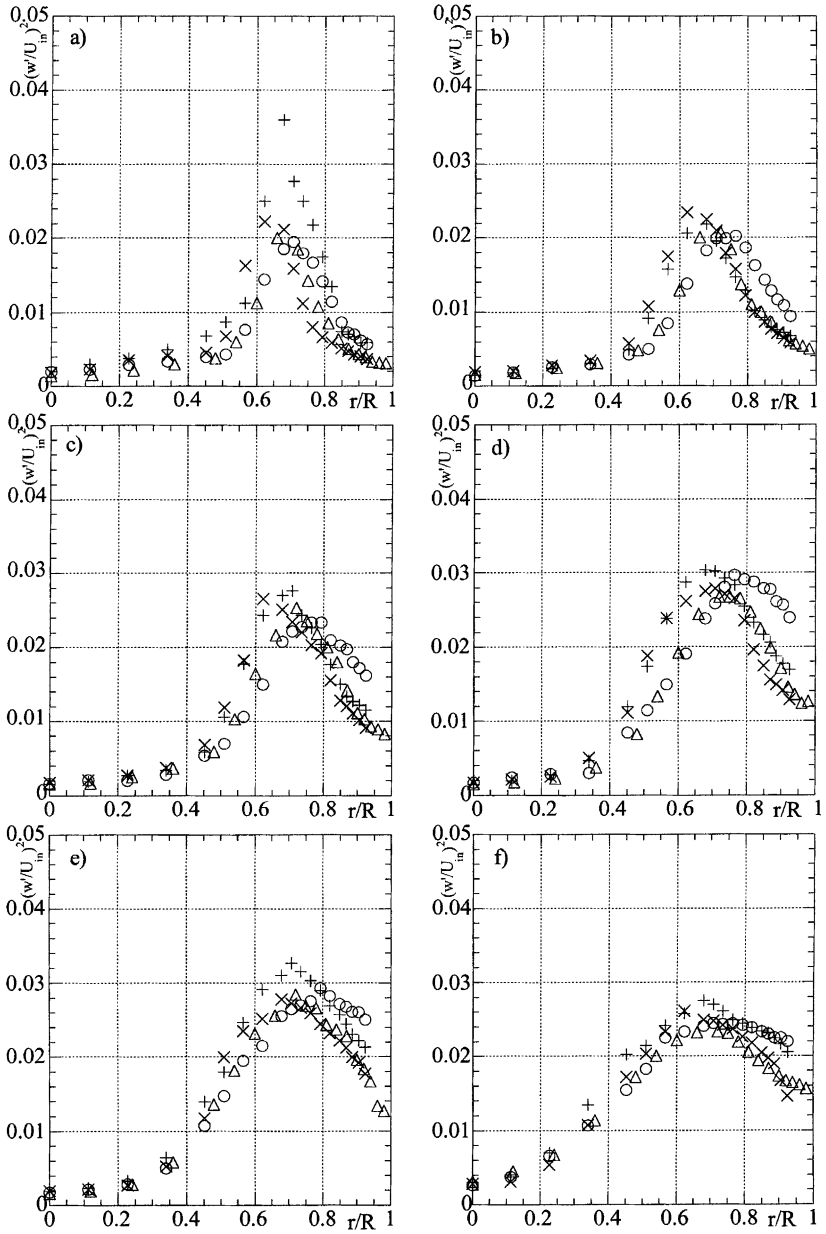

Fig. 8. Transverse profiles of the tangential normal Reynolds stress downstream of the expansion for (×) water $Re = 50{,}300$; (+) water $Re = 135{,}000$; (△) 1% laponite $Re_w = 48{,}160$; (○) 1% laponite $Re_w = 99{,}540$ at $x =$ (a) $0.5d$; (b) $0.75d$; (c) $1.0d$; (d) $1.5d$; (e) $2.0d$; (f) $3.0d$.

These measurements were carried out at high Reynolds numbers, in a range where Reynolds number effects are absent from sudden expansion flow characteristics, at least for Newtonian fluids. Therefore, there is here no major consequence regarding any controversy about the relationship between the true condition of the flow of this thixotropic suspension and its equilibrium behaviour in the rheological

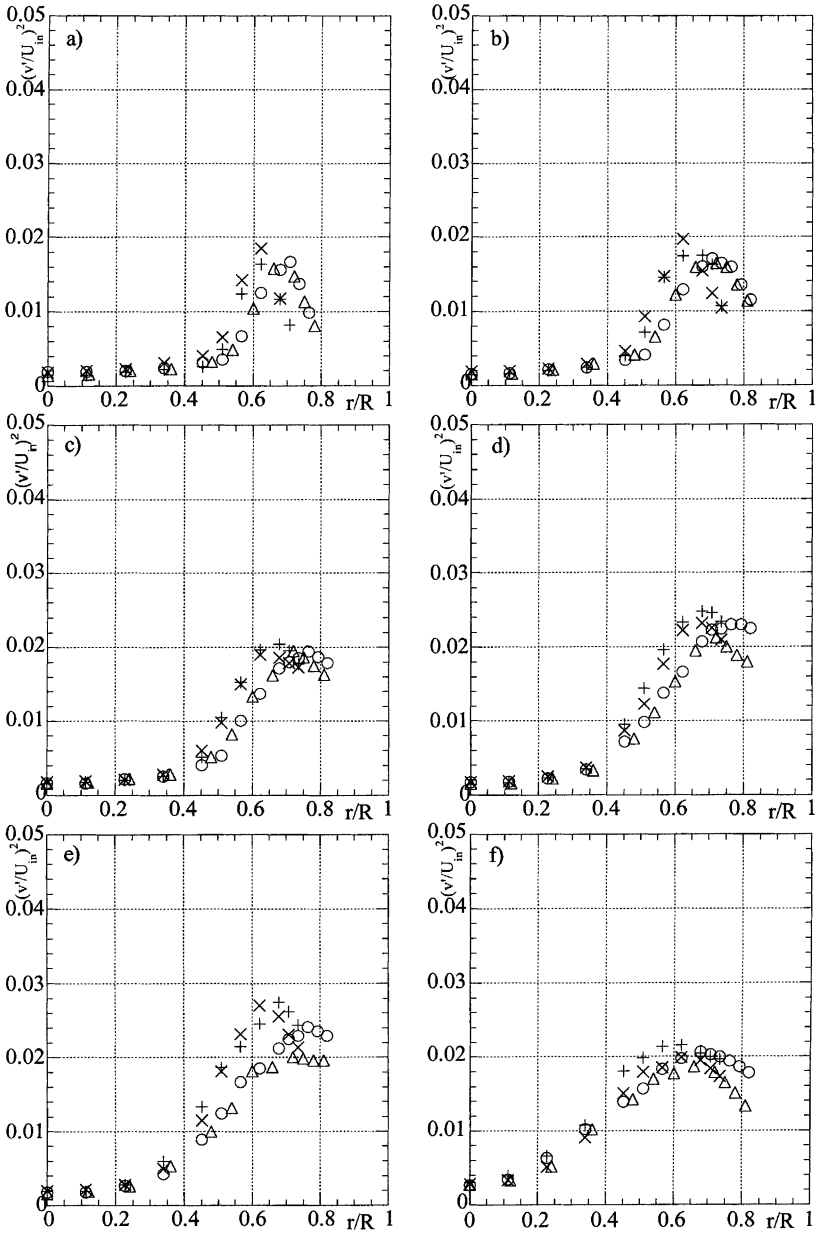

Fig. 9. Transverse profiles of the radial normal Reynolds stress downstream of the expansion for (×) water $Re = 50{,}300$; (+) water $Re = 135{,}000$; (△) 1% laponite $Re_w = 48{,}160$; (○) 1% laponite $Re_w = 99{,}540$ at $x =$ (a) $0.5d$; (b) $0.75d$; (c) $1.0d$; (d) $1.5d$; (e) $2.0d$; (f) $3.0d$.

characterisation. However, it is obvious that the equilibrium condition in the sudden expansion flow must necessarily be different from the equilibrium condition in the flow curve of the previous section. In this sudden expansion flow, the laponite suspensions behaved as purely viscous fluids and did not exhibit any strange behaviour that could be attributed to fluid elasticity.

5. Conclusions

A detailed investigation of the rheology of a pure clay suspension, and its turbulent flow characteristics in a sudden expansion, were carried out. The aqueous suspension of clay was based on laponite RD from Laporte Industries and was made at a weight concentration of 1%.

The fluid was shear-thinning and thixotropic, so the measurement of the viscometric viscosity had to follow an equilibrium procedure. The fluid also exhibited an yield stress which was measured by two direct methods and curve fitting by two known viscosity models. It was the value of 0.9 Pa, obtained by the latter indirect methods, that was considered adequate for the analysis of hydrodynamic results. The oscillatory shear flow test showed that the 1% laponite suspension was almost inelastic.

The results of the turbulent flow downstream of a sudden expansion, at wall Reynolds numbers in excess of 40,000 and fully-developed inlet flow conditions, were consistent with the straight pipe flow measurements of [19] as well as with the measurements taken at the inlet pipe. First, there were no differences between the laponite and water mean and turbulent flow characteristics in the upstream fully-developed pipe flow, which could then be advected and influence the downstream flow. Secondly, there were also no major differences between the downstream flows of water and of the laponite suspension, i.e. the suspension behaved as a purely viscous fluid. The slight anticipation of the loci of maximum Reynolds stresses seen with laponite was not sufficiently intense to affect the mean and turbulent flows downstream of that location, in a manner that is different to that of the water flows.

Acknowledgements

The authors acknowledge the financial support of the Stichting Fund of Schlumberger. The laboratory facilities provided by INEGI — Instituto de Engenharia Mecâmca e Gestão Industrial — were fundamental for the successful outcome of this work. Helpful discussions with Prof. M.P. Escudier of the University of Liverpool are also acknowledged.

References

[1] J. Mewis, Thixotropy — a general review, J. Non-Newtonian Fluid Mech. 6 (1979) 1–20.
[2] M.P. Escudier, F. Presti, Pipe flow of a thixotropic liquid, J. Non-Newtonian Fluid Mech. 62 (1996) 291–306.
[3] S.B. Pope, Turbulent Flows, Cambridge University Press, Cambridge, 2000.
[4] R.P. Durrett, W.H. Stevenson, H.D. Thompson, Radial and axial turbulent flow measurements with an LDV in an axisymmetric sudden expansion air flow, ASME J. Fluids Eng. 110 (1988) 367–372.
[5] M. Stieglmeier, C. Tropea, N. Weiser, W. Nitsche, Experimental investigation of the flow through an axisymmetric sudden expansion, ASME J. Fluids Eng. 111 (1989) 464–471.
[6] W.J. Devenport, E.P. Sutton, An experimental study of two flows through an axisymmetric sudden expansion, Exp. Fluids 14 (1993) 423–432.
[7] O.S. Castro, F.T. Pinho, Turbulent expansion flow of low molecular weight shear-thinning solutions, Exp. Fluids 20 (1995) 42–55.
[8] M.P. Escudier, S. Smith, Turbulent flow of Newtonian and shear-thinning liquids through a sudden axisymmetric expansion, Exp. Fluids 27 (1999) 427–434.
[9] J.H. Iwamiya, A.W. Chow, S.W. Sinton, NMR flow imaging of Newtonian liquids and a concentrated suspension through an axisymmetric sudden contraction, Rheol. Acta 33 (1994) 267–282.
[10] Laponite, 90 Laponite Technical Bulletin L106/90/C, Laporte Inorganics, Cheshire, UK.

[11] S. Cocard, T. Nicolai, J.-F. Tassin, Thixotropic behaviour of laponite suspensions as studied by rheo-optical techniques, in: Proceedings of the XIIIth International Congress on Rheology, Vol. 4, Cambridge, UK, 2000, pp. 160–162.
[12] J.T. Park, R.T. Mannheimer, T.A. Grimley, T.B. Morrow, Pipe flow measurements of a transparent non-Newtonian slurry, ASME J. Fluids Eng. 111 (1989) 331–336.
[13] M.P. Escudier, D.M. Jones, I.W. Gouldson, Fully-developed pipe flow of shear-thinning liquids, in: Proceedings of the Sixth International Symposium on Applications of Laser Techniques to Fluid Mechanics, Lisbon, Paper 1.3, 1992.
[14] J. Laufer, The structure of turbulence in fully-developed pipe flow, NACA report 1174, 1954.
[15] B. Pak, Y.I. Cho, S.U. Choi, Separation and reattachment of non-Newtonian fluid flows in a sudden expansion pipe, J. Non-Newtonian Fluid Mech. 37 (1990) 175–199.
[16] B. Pak, Y.I. Cho, S.U. Choi, Turbulent hydrodynamic behaviour of a drag reducing viscoelastic fluid in a sudden expansion pipe, J. Non-Newtonian Fluid Mech. 39 (1991) 353–373.
[17] A.S. Pereira, F.T. Pinho, Turbulent characteristics of shear-thinning fluids in recirculating flows, Exp. Fluids 28 (2000) 266–278.
[18] A.S. Pereira, F.T. Pinho, The effect of the expansion ratio on a turbulent non-Newtonian recirculating flow, Exp. Fluids, 2000, submitted for publication.
[19] A.S. Pereira, F.T. Pinho, Turbulent pipe flow of thixotropic fluids, Int. J. Heat Fluid Flow, 2001, submitted for publication.
[20] R. Shaw, The influence of hole dimensions on static pressure measurements, J. Fluid Mech. 7 (1960) 550–564.
[21] R.E. Franklin, J.M. Wallace, Absolute measurements of static-hole error using flush transducers, J. Fluid Mech. 42 (1970) 33–48.
[22] M. Stieglmeier, C. Tropea, A miniaturised, mobile laser–Doppler anemometer, Appl. Opt. 31 (1992) 4096.
[23] F. Durst, A. Melling, J.H. Whitelaw, Principles and Practice of Laser–Doppler Anemometry, 2nd Edition, Academic Press, New York, 1981.
[24] Laponite, L104, Laponite: structure, chemistry and relationship to natural clays, Laponite Technical Bulletin L104/90/A, Laporte Absorbents, Cheshire, UK.
[25] Laponite, Laponite: structure, chemistry and relationship to natural clays, Laponite Technical Bulletin L104/90/A, Laporte Absorbents, Cheshire, UK, 1990.
[26] N.J. Alderman, D. Ram Babu, T.L. Hughes, G.C. Maitland, The rheological properties of water-based drilling fluids, in: Proceedings of the Xth International Congress on Rheology, Sydney, 1988, pp. 140–142.
[27] D.C.-H. Cheng, Yield stress: a time-dependent property and how to measure it, Rheol. Acta 25 (1986) 542–554.
[28] R.A. Speers, K.R. Hilme, M.A. Tung, W.T. Williamson, Drilling fluid shear stress overshoot behaviour, Rheol. Acta 26 (1987) 447–452.
[29] P.V. Liddell, D.V. Boger, Yield stress measurements with the vane, J. Non-Newtonian Fluid Mech. 63 (1996) 253–261.
[30] C.J. Lawn, The determination of the rate of dissipation in turbulent pipe flow, J. Fluid Mech. 48 (1971) 477–505.
[31] H.W. Townes, J.L. Gow, R.E. Powe, N. Weber, Turbulent flow in smooth and rough pipes, J. Basic Eng. 94 (1972) 353–362.
[32] J.A. Clark, A study of incompressible turbulent boundary layers in channel flow, J. Basic Eng. 90 (1968) 455–468.
[33] F.T. Oliveira, F.T. Pinho, Pressure drop coefficient of laminar Newtonian flow in axisymmetric sudden expansions, Int. J. Heat Fluid Flow 18 (1997) 518–529.